THE JOURNAL OF BIOLOGICAL CHEMISTRY VOL. 282, NO. 22, pp. 16441–16453, June 1, 2007

Ataxia Telangiectasia Mutated (ATM) Signaling Network Is Modulated by a Novel Poly(ADP-ribose)-dependent Pathway in the Early Response to DNA-damaging Agents*[S]

Received for publication, August 31, 2006, and in revised form, April 10, 2007 Published, JBC Papers in Press, April 11, 2007, DOI 10.1074/jbc.M608406200

Jean-François Haince[‡1], Sergei Kozlov[§], Valina L. Dawson[¶2], Ted M. Dawson[¶2,3], Michael J. Hendzel[‖], Martin F. Lavin[§], and Guy G. Poirier[‡4]

From the [‡]Health and Environment Unit, Laval University Hospital Research Center, CHUQ, Faculty of Medicine, Laval University, Quebec, Quebec G1V 4G2, Canada, the [§]Queensland Institute for Medical Research, PO Royal Brisbane Hospital, Brisbane, Queensland 4029, Australia, the [¶]Institute for Cell Engineering and the Departments of Neurology and Neuroscience, The Johns Hopkins University School of Medicine, Baltimore, Maryland 21205, and the [‖]Department of Oncology, Faculty of Medicine, University of Alberta and Cross Cancer Institute, Edmonton, Alberta T6G 1Z2, Canada

Poly(ADP-ribosyl)ation is a post-translational modification that is instantly stimulated by DNA strand breaks creating a unique signal for the modulation of protein functions in DNA repair and cell cycle checkpoint pathways. Here we report that lack of poly(ADP-ribose) synthesis leads to a compromised response to DNA damage. Deficiency in poly(ADP-ribosyl)ation metabolism induces profound cellular sensitivity to DNA-damaging agents, particularly in cells deficient for the protein kinase ataxia telangiectasia mutated (ATM). At the biochemical level, we examined the significance of poly(ADP-ribose) synthesis on the regulation of early DNA damage-induced signaling cascade initiated by ATM. Using potent PARP inhibitors and PARP-1 knock-out cells, we demonstrate a functional interplay between ATM and poly(ADP-ribose) that is important for the phosphorylation of p53, SMC1, and H2AX. For the first time, we demonstrate a functional and physical interaction between the major DSB signaling kinase, ATM and poly(ADP-ribosyl)ation by PARP-1, a key enzyme of chromatin remodeling. This study suggests that poly(ADP-ribose) might serve as a DNA damage sensory molecule that is critical for early DNA damage signaling.

Double-strand breaks (DSB)[5] are potentially the most cytotoxic form of DNA damage in human cells because they lead to genomic rearrangements, cancer predisposition, and perhaps cell death if unrepaired or repaired incorrectly (1). Consequently, the DNA damage response involves parallel modulation of redundant signaling pathways leading to lesion detection, processing, and repair. Ataxia telangiectasia mutated (ATM) is a DNA damage-responding kinase that is rapidly activated after the induction of DSB (2). Within minutes of DNA damage induction, ATM is recruited and activated in the vicinity of DSBs, where it induces the phosphorylation of a number of proteins required for DNA damage response and repair, including proteins of MRN (Mre11/Rad50/NBS1) complex, p53, SMC1 and histone variant H2AX (3). However, the detailed mechanisms of how ATM is activated and regulates its downstream effectors are not fully understood. Although ATM activation is mainly associated with DSB formation as part of the damage detection mechanism following ionizing radiation (IR), several studies indicate that the signaling kinase ATM is also activated in response to the environmental carcinogen *N*-methyl-*N*′-nitro-*N*-nitrosoguanidine (MNNG) (4–6).

Poly(ADP-ribose) polymerases (PARPs) are also constitutive factors of the DNA damage surveillance network, acting through a DNA break sensor function (7). Several observations indicate that poly(ADP-ribosyl)ation also plays an early role in DSB signaling and repair pathways (8–11). PARP-1 and PARP-2 are highly activated upon binding to DNA strand interruptions and synthesize, within seconds, large amounts of the negatively charged polymer of ADP-ribose (PAR) on several nuclear proteins including themselves, histones, topoisomerase I, and DNA-dependent protein kinase (DNA-PK) (12). The immediate activation of PARP-1 by DNA breaks and the resulting PAR build-up, which appears minutes after DNA damage induction, are among the earliest cell responses to DNA damage (13–15). After initial recruitment of PARP-1 to DNA lesions, hyperpoly(ADP-ribosyl)ated PARP-1 dissociates from the DNA template (16), leading to relaxation of chromatin structure (17), which may facilitate the recruitment of repair proteins to damaged sites via direct interactions with PAR (18). Furthermore, multiple reports show that PARP inhibitors

* This work was supported by the Canadian Institutes of Health Research (CIHR). The costs of publication of this article were defrayed in part by the payment of page charges. This article must therefore be hereby marked "*advertisement*" in accordance with 18 U.S.C. Section 1734 solely to indicate this fact.

[S] The on-line version of this article (available at http://www.jbc.org) contains supplemental Figs. S1 and S2.

[1] Supported by a scholarship from the CIHR Strategic Training Program Grant in Genomics, Proteomics, and Bioinformatics.

[2] Supported by NINDS, National Institutes of Health Grant NS39148.

[3] The Leonard and Madlyn Abramson Professor in Neurodegenerative Diseases.

[4] Holds a Canada Research Chair in Proteomics. To whom correspondence should be addressed: CHUL Rm. RC-9700, 2705, Laurier Blvd., Quebec, Quebec G1V 4G2, Canada. Tel.: 418-654-2267; Fax: 418-654-2159; E-mail: guy.poirier@crchul.ulaval.ca.

[5] The abbreviations used are: DSB, DNA double-strand break; ATM, ataxia telangiectasia mutated; MRN, Mre11/Rad50/NBS1; SMC1, structural maintenance of chromosomes 1; IR, ionizing radiation; MNNG, *N*-methyl-*N*′-nitro-*N*-nitrosoguanidine; PAR, poly(ADP-ribose); PARP, poly(ADP-ribose) polymerase; PARG, poly(ADP-ribose) glycohydrolase; DNA-PK, DNA-dependent protein kinase; ATR, A-T and RAD-3-related; MEF, mouse embryonic fibroblast; A-T, ataxia-telangiectasia; Gy, Gray; GST, glutathione *S*-transferase.

increase the cytotoxicity of DNA-damaging agents and IR (19–21). This is manifested by a delay in the progression through the S phase and accumulation of cells in G_2/M (22, 23). Although viable, both PARP-1 and PARP-2 knock-out mice display an acute sensitivity to IR and alkylating agents (24, 25). PARP-1/PARP-2 double knock-out mice die at early stages of embryogenesis, demonstrating the crucial functions of poly(ADP-ribosyl)ation in DNA damage signaling and the existence of functional redundancy between these two PARPs (25). Interestingly, PARP-1/ATM double mutant mice are defective for both repair and signaling of DNA damage, leading to embryonic lethality because of their dramatic sensitivity to DNA damage (26, 27).

Recently, the notion that PAR mediates key events in cell cycle regulation such as mitotic spindle control through PAR binding interaction (28–30) stimulated our interest on the possible role of PAR-binding proteins in early DNA damage response and specifically the interplay between the signaling kinase ATM and PAR molecules. A number of proteins involved in DNA damage signaling contain modular domains that mediate specific protein-protein interactions. Consequently, a PAR-binding domain has been found in a number of proteins involved in DNA damage response pathways such as p53, p21, XRCC1, Ku70, topoisomerase I, and DNA ligase IIIα (31–34). However, despite major advances primarily by biochemical and genetic studies, the precise role of poly(ADP-ribosyl)ation in the immediate DNA damage signaling remains to be elucidated. The finding that ATM is activated, at least *in vitro*, by PAR molecules (35) raises the issue as to whether PAR influences the phosphorylation cascade initiated by the ATM protein kinase.

In this study, we determined how PAR synthesis modulated the early DNA damage signaling response. We show that impaired PAR synthesis in cells treated with the PARP inhibitors is associated with delayed phosphorylation of p53, H2AX, and SMC1 after DNA damage caused by treatment with both MNNG and IR. The decreased phosphorylation and stabilization of p53 and delayed phosphorylation of SMC1 and histone H2AX were also confirmed in mouse embryonic fibroblasts (MEFs) derived from PARP-$1^{-/-}$ mice. In addition, we demonstrate that PAR interacts physically with ATM, that this interaction is mediated by PAR-binding domains and that it has functional consequences.

MATERIALS AND METHODS

Cell Lines—The human lung adenocarcinoma cells (A549) (ATCC CCL-185) were maintained in Ham's F12K medium with 2 mM glutamine containing 15% fetal bovine serum, penicillin (100 units/ml), and streptomycin (100 μg/ml). SV40-transformed normal skin fibroblasts (GM00637), and A-T fibroblasts (GM09607) as well as mouse embryonic fibroblasts derived from PARP-$1^{+/+}$ (F20) and PARP-$1^{-/-}$ (A1) mice (36) were grown in Dulbecco's modified Eagle's medium supplemented with 10% fetal bovine serum, glutamine (2 mM), penicillin (100 units/ml), and streptomycin (100 μg/ml). Alternatively, the EBV-immortalized normal lymphoblastoid cells (C3ABR) and A-T lymphoblastoid cells (GM03189) were used and maintained in RMPI 1640 medium supplemented with 15% fetal bovine serum, glutamine (2 mM), penicillin (100 units/ml), and streptomycin (100 μg/ml).

Immunoprecipitation, Western Blotting, and Antibodies—We exposed control and A-T cells to genotoxic agents (MNNG and IR) and collected whole cell extracts at the indicated time points as described (37). We performed precipitation of endogenous PARP-1 with an anti-PARP-1 monoclonal antibody (F1–23). Cells were resuspended in 25 mM $NaPO_4$ buffer pH 8, 150 mM NaCl, 1 mM EDTA, 0.2% Nonidet P-40, 1 mM dithiothreitol, 1 mM phenylmethylsulfonyl fluoride, and protease inhibitors Complete^{TM} (Roche Applied Science) and kept on ice for 20 min. $NaPO_4$ and NaCl concentration were then adjusted to 175 mM (150 μl/ml) and 0.3 M (30 μl/ml), respectively, and homogenized using a Dounce homogenizer with 30 strokes with the tight-fitting pestle. A suspension of magnetic protein G beads (Invitrogen) was washed twice with binding buffer (175 mM $NaPO_4$, pH 8.0 containing 150 mM NaCl, 1 mM EDTA, 0.5 mM phenylmethylsulfonyl fluoride, 1 mM dithiothreitol, and protease inhibitors) prior to immunoprecipitation. Cleared lysate was diluted to 1:2 (v/v) with binding buffer without NaCl, mixed with the antibody-coated beads, and incubated with rotation at 4 °C for 90–120 min. The beads were washed with the binding buffer. The beads containing the immunoprecipitated samples were collected, resuspended in 250 μl of SDS loading buffer and boiled 5 min at 100 °C. Whole cell extracts (10 μg) or immunoprecipitates were analyzed by SDS-PAGE and electrotransferred onto nitrocellulose membranes. Immunoblots were probed with antibodies directed against PAR (96–10 antisera), PARP-1 (clone C2–10), p53 protein, p53 phospho-S15, SMC1 phospho-S957, SMC1 (Cell Signaling), H2AX phospho-S139 (Upstate), and β-actin (Calbiochem). Immunoblots were developed using the Super Signal West Dura Extended Duration (Pierce) to allow quantitative analysis.

Purification of GST-ATM Fragments and in Vitro Pull-down Assays—For *in vitro* PAR binding characterization, we prepared a series of GST-ATM constructs as described (38). For the GST pull-down, glutathione-Sepharose beads (80 μl) were washed with lysis buffer and then resuspended in 400 μl of lysis buffer containing either purified GST-tagged ATM domains (1 μg) or GST protein alone. For each condition, PARP-1 (1 μg), ^{32}P-modified PARP-1 (100 nM), PARG (1 unit), or PAR (100 nM) were added to the reaction mixture. After a 2-h incubation at 4 °C with constant mixing, the beads were washed extensively in lysis buffer containing 500 mM NaCl. The beads were collected by centrifugation, resuspended in 250 μl of SDS loading buffer and boiled 5 min at 100 °C. After separation by SDS-PAGE, bound material was detected by autoradiography, immunoblotting with anti-PARP-1 (clone C2–10) or Coomassie Blue staining.

Nitrocellulose PAR Binding Assay—Synthetic peptides or purified proteins were loaded onto a nitrocellulose membrane (0.1 μm pore size) using a dot blot manifold system. Membranes were incubated with ^{32}P-labeled automodified PARP-1 or ^{32}P-labeled purified PAR prepared as described (39), washed extensively, and subjected to autoradiography.

BioPorter-mediated Delivery of Peptides into Cells—Wild-type and mutant ATM N-terminal PAR-binding peptides were

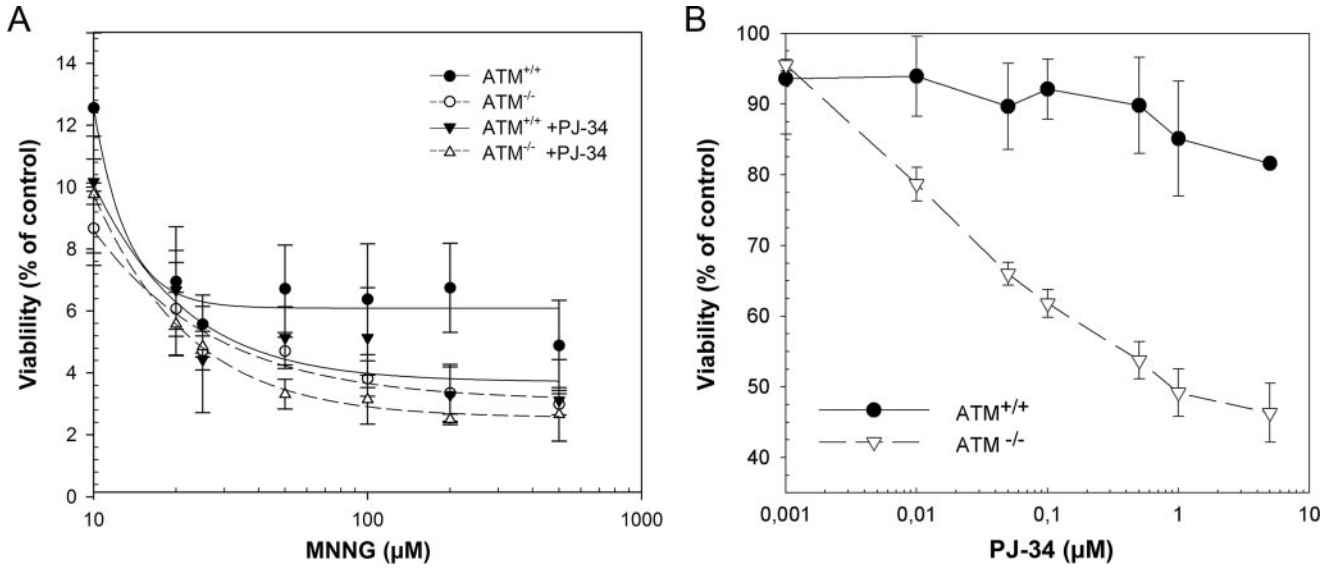

FIGURE 1. **Normal and A-T cells are hypersensitive to MNNG-induced DNA damage in the absence of poly(ADP-ribosyl)ation.** *A*, viability of normal lymphoblastoid cells (C3ABR) and lymphoblastoid cells derived from an A-T patient (GM03189) treated with increasing concentrations of MNNG alone or in combination with 5 μM PJ-34 was evaluated as described under "Materials and Methods." *B*, cell survival was also determined after exposure to increasing concentrations of PJ-34 to establish its relative cytotoxicity. Data are the mean ± S.E. from three independent experiments.

delivered into cells using the BioPorter reagent (Sigma) (40, 41). Purified peptides were diluted to the desired concentration in PBS. The diluted peptide solution (2.5 μg of total) was added to the dried BioPorter reagent and allowed to sit at room temperature for 5 min followed by gentle mixing. The suspensions were mixed with 250 μl of serum-free medium and were then added to cells (~60–80% confluency) cultured in 6-well cell culture plates for 3–4 h at 37 °C. Cultures were subsequently used for experiments.

Cytotoxicity Studies—Cells were suspended in RPMI 1640 medium and plated out at 2×10^5 cells/ml in 24-well cell culture plates. Cells were exposed for 1 h to a range of concentrations of the PARP inhibitor PJ-34 (Axxora) or a range of MNNG concentrations in growth medium. After treatment, fresh media with or without PJ-34 was added, and plates were incubated for 4–5 days at 37 °C in a 10% CO_2 incubator until untreated control cells reached ~2×10^6 cells/ml. Cell viability (triplicate wells for each drug concentration) was determined by adding 0.1 ml of 0.4% Trypan blue to a 0.5-ml cell suspension (42). Viable cells were counted, and viabilities were expressed as the number of cells in drug-treated wells relative to cells in control wells (% of control).

Immunofluorescence and Microscopy Analysis—A549 or GM00637 cells were fixed at the indicated time points following treatment with DNA-damaging agents (MNNG or IR). PAR synthesis was detected with the rabbit anti-PAR 96–10 antibody. Nuclear foci of DNA damage were visualized using anti-H2AX pS139 monoclonal antibody (Upstate). Cells were observed using a Zeiss microscope (Axioplan IIM) equipped with a CoolSnapHQ cooled CCD camera. The measurement of fluorescence intensity and colocalization was performed using MetaMorph 6.0 (Universal Imaging) software. Composite figures of collected images were assembled in Adobe Photoshop.

Confocal Microscopy and Quantification of γ-H2AX Foci—To detect MNNG-induced γ-H2AX foci, PARP-$1^{+/+}$ and PARP-$1^{-/-}$ MEF grown on coverslips were fixed at various time points after MNNG exposure and stained with anti-H2AX pS139 monoclonal antibody. Cells labeled as described above were placed on a Nikon inverted confocal laser-scanning microscope and images were captured using the LaserSharp software. The number of γ-H2AX foci per cell were manually counted in three separate fields (at least 50 cells/fields). Cells were classified into four different categories according to the number of γ-H2AX foci per cell (0–5, 5–15, 15–30, or more than 30 foci per cell).

Cell Cycle Analysis—Cell cycle distribution after PJ-34 and MNNG treatments was determined by flow cytometry analysis using propidium iodine staining for DNA content. Cell death was characterized by the number of cells with fragmented DNA (sub-G_1 population).

RESULTS

Loss of PAR Synthesis Sensitizes Normal Cells to DNA-damaging Agents—Genetic disorders that cause deficiency in DNA damage signaling proteins are characterized by an increased sensitivity to a variety of DNA-damaging agents. Cells derived from patients with Ataxia-Telangiectasia (A-T) illustrate perfectly this paradigm showing a defective response to DNA damage (43). Similarly, it has been demonstrated that disruption of PAR synthesis causes an increase in sensitivity to DNA-damaging agents (21), suggesting that deficiency in PAR metabolism is linked to a defect in DNA damage signaling. Thus, to determine whether the effects of PARP inhibition impacts on the ATM signaling network, we compared the sensitivity to DNA alkylating agents in normal ATM-proficient lymphoblasts and in A-T patient cells. As shown in Fig. 1*A*, normal cells exposed for one hour to both MNNG and PARP inhibitors exhibit survival rates similar to A-T cells treated with MNNG alone, suggesting that the absence of PAR synthesis decreases the ability of normal cells to respond adequately to DNA damage to an extent similar to that observed in A-T cells.

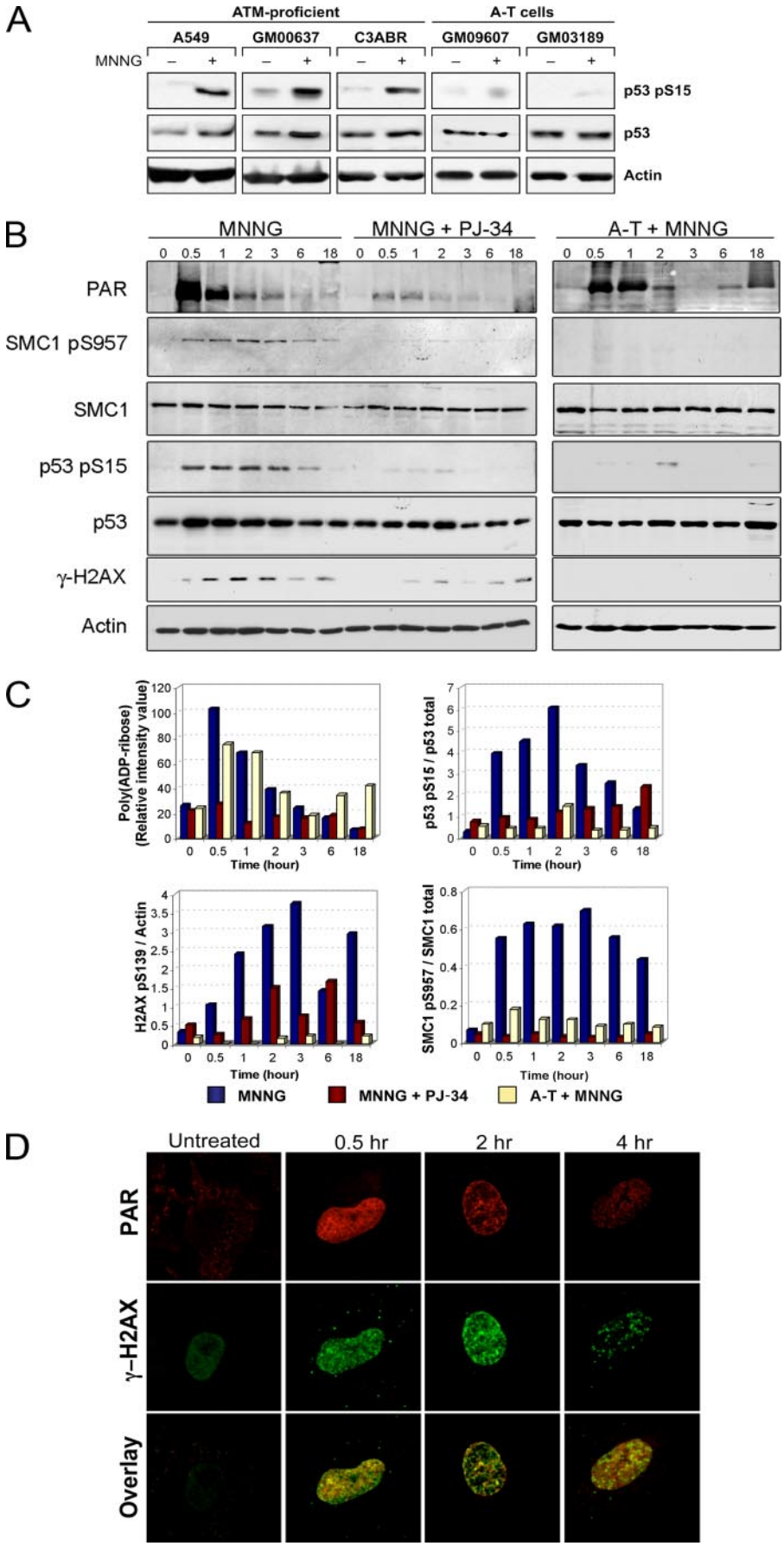
A
ATM-proficient
A-T cells
A549
GM00637
C3ABR
GM09607
GM03189
MNNG
p53 pS15
p53
Actin
B
MNNG
MNNG + PJ-34
A-T + MNNG
PAR
SMC1 pS957
SMC1
p53 pS15
p53
γ-H2AX
Actin
C
Poly(ADP-ribose) (Relative intensity value)
p53 pS15 / p53 total
H2AX pS139 / Actin
SMC1 pS957 / SMC1 total
Time (hour)
MNNG
MNNG + PJ-34
A-T + MNNG
D
Untreated
0.5 hr
2 hr
4 hr
PAR
γ–H2AX
Overlay

We next evaluated whether PJ-34 exhibits inhibitor-specific toxicity in the absence of treatment with exogenous cytotoxic drugs using survival as readout (Fig. 1*B*). We observed a relatively low toxicity in normal ATM-proficient cells when low doses of PJ-34 were added to growth medium (Fig. 1*B*). However, A-T cells are acutely sensitive to treatment with the same low doses of PJ-34 (Fig. 1*B*). This finding is consistent with previous reports showing that deficiency in DNA damage signaling proteins induces sensitivity to PARP inhibition (10, 26). We also established that the hypersensitivity of A-T cells to the suppression of PARP-1 function is due to the activation of apoptosis (supplemental Fig. S1). This is illustrated by the increased sub-G_1 population (supplemental Fig. S1B) and the appearance of the specific PARP-1 cleavage product (supplemental Fig. S1C). Together, these results clearly show that disruption of PARP function by chemical inhibition in normal cells leads to the suppression of an important signaling event of the DNA damage response that is comparable to the cell survival defect observed in cells lacking ATM.

MNNG Induces ATM-dependent Substrate Phosphorylation That Is Altered in the Absence of PAR Synthesis—The DNA damage-responsive kinase ATM is best known for its activation following IR (2). Besides, ATM has also been proven to be the main kinase responsible for the phosphorylation of p53 on serine 15 during MNNG-induced DNA damage (4). In addition, it was shown that NBS1, SMC1, and p53 were phosphorylated in an ATM-dependent manner at high doses of MNNG-induced DNA strand breaks, while ATR responds to the formation of DNA adducts and stalled replication induced by UV radiation (4–6). We have analyzed this specific phosphorylation of p53 using a large panel of normal ATM-proficient and A-T cell lines. All ATM-proficient cells show induction of p53 phosphorylation 1 h after MNNG treatment (Fig. 2*A*). In contrast, negligible signal was detected in both A-T cell lines exposed to the same treatment (Fig. 2*A*). Taken together, these findings confirm that high MNNG doses activate the ATM kinase, which allow the direct and rapid phosphorylation of p53 on serine 15 (4, 6). Therefore, we used MNNG to activate both ATM protein kinase and PAR formation to establish the relationship between ATM and PARP-1.

We hypothesized that PAR molecules might influence ATM function, either by promoting its kinase activity or by providing access to its downstream substrates. Recent studies have demonstrated that ATM kinase activity is significantly enhanced by PAR (35). Because poly(ADP-ribosyl)ation occurs with kinetics similar to that of ATM activation during initial steps of the DNA damage signaling (27), it is therefore conceivable that PAR could trigger ATM phosphorylation of a subset of its targets within the first hour after DNA breaks formation. To understand the mechanism of PARP-1 activation in response to MNNG, we first determined the time-course of PARP activation in normal and A-T cells as well as in PARP-inhibited cells exposed to 50 μM MNNG (Fig. 2*B*). Exposure of both normal and A-T cells to MNNG results in an immediate synthesis of PAR that peaks at 30 min post-treatment, and rapidly decreases after 1 h, demonstrating how fast the PAR-dependent response can be (Fig. 2, *B* and *C*). However, in cells exposed to a 5 μM dose of PJ-34, we observed a striking inhibition (98.5%) of PAR synthesis following MNNG exposure (Fig. 2, *B* and *C*). Having observed that DNA damage-dependent PAR synthesis follows rapid kinetics in both normal and A-T cells, we next examined the ATM-dependent response within the same time frame following treatment with both MNNG and PJ-34. We performed biochemical analysis on the well-established ATM substrates p53, SMC1, and H2AX using phosphospecific antibodies. Importantly, cells treated with both MNNG and PJ-34 present a 5-fold decrease of p53 phosphorylation at 30 min and 1 h post-treatment (Fig. 2*B*-C). Pretreatment of the cells with PJ-34 significantly reduced the MNNG-induced phosphorylation of SMC1 on serine 957 throughout the treatment (Fig. 2, *B* and *C*). Next we used an ATM-deficient cell line to determine whether the phosphorylation cascade induced by MNNG is dependent of the protein kinase ATM. Although these cells demonstrate normal level of PAR synthesis following MNNG exposure, they exhibit a defective phosphorylation of ATM-dependent substrates p53, SMC1 and H2AX (Fig. 2, *B* and *C*). Besides, no phosphorylation of p53 and SMC1 was observed in the ATM-deficient cells when PAR synthesis peaks (>1 h). This indicates that PAR could not signal directly to other members of the PI3K kinase family such as ATR and DNA-PK. Importantly, we found that treatment of A-T lymphoblasts with MNNG greatly attenuated the phosphorylation of p53 and SMC1 in initial time points, which demonstrated that the protein kinase ATM is responsible phosphorylation of these effectors following MNNG exposure. Together these results suggest that the absence of PAR modulates the ATM-dependent phosphorylation of numerous downstream effectors including p53 and SMC1 immediately after MNNG exposure. Similar effects were also observed with another PARP inhibitor, DPQ (supplemental Fig. S2). In these cells, over 90% of the PAR synthesis was inhibited 1 h after treatment (data not shown) and the MNNG-induced phosphorylation of p53 is about 60% of that measured when PAR is fully synthesized (supplemental Fig. S2). These results indicate that the reduced phosphorylation of p53 is due to the absence of PAR rather than a PJ-34 specific effect.

The ability of γ-H2AX to form nuclear foci upon DNA damage has long been recognized as a sensitive marker of DSB formation (44, 45). Consequently, we noticed a 26% reduction of

FIGURE 2. **Disruption of PAR synthesis affects the MNNG-induced DNA damage response.** *A*, panel of ATM-proficient (A549, GM00637, C3ABR) cells along with ATM-deficient (GM09607, GM03189) cells were treated with MNNG (50 μM) for 1 h and harvested. The phosphorylation state of p53 on serine 15 was analyzed by Western blotting using a phosphospecific antisera. The immunoblots were then probed for total p53 and actin. *B*, A549 cells were pretreated or not for 1 h with PJ-34 (5 μM) prior to addition of MNNG (50 μM) and compared with ATM-deficient cells (GM03189) treated with the same dose of MNNG. Total cell extracts were prepared at indicated time points following MNNG exposure and immunoblotted with antibodies directed against PAR (pAb 96-10), phospho-SMC1 (serine 957), SMC1, phospho-p53 (serine 15), p53, γ-H2AX, and actin (loading control). *C*, quantification of PAR synthesis, p53 phosphorylation on serine 15, γ-H2AX and SMC1 phosphorylation on serine 957 were performed directly on immunoblots shown in *B*. *D*, A549 cells were immunostained with anti-PAR polyclonal antibody 96-10 and anti-γH2AX monoclonal antibody at the indicated time points following 50 μM MNNG treatments. *Bottom panel*s show co-localization of γ-H2AX foci with sites of PAR synthesis. Data are representative of at least three independent experiments.

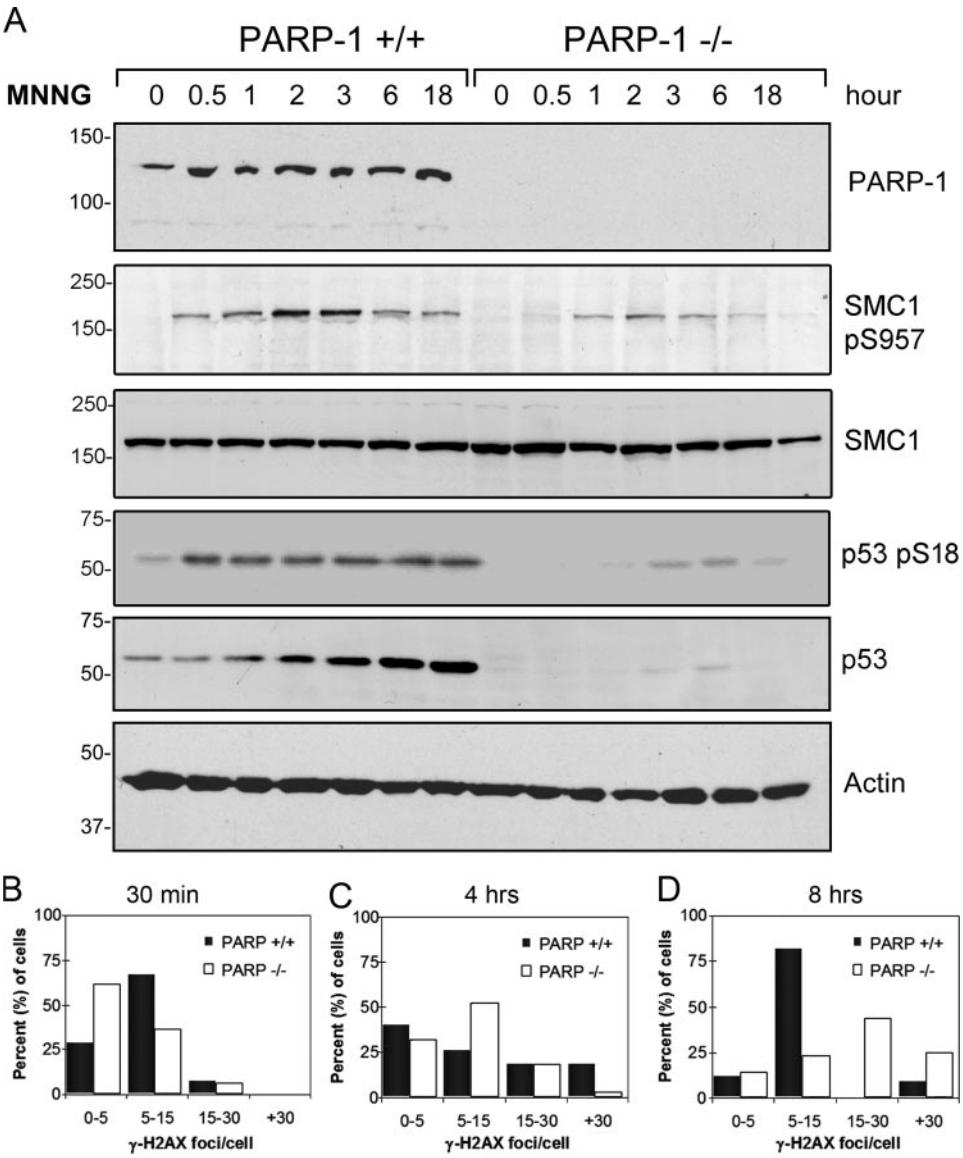

FIGURE 3. **PARP-1-deficient cells have impaired p53 stabilization and defective γ-H2AX foci formation.** *A*, total extract from wild type (PARP-$1^{+/+}$) and knock-out (PARP-$1^{-/-}$) MEFs were immunoblotted against PARP-1, phospho-SMC1 (serine 957), SMC1, phospho-p53 (serine 18 in mice), and p53 at the indicated time points following 50 μM MNNG treatments. PARP-1 status was assessed by Western blot using PARP-1 antibody and equal gel loading was verified using an anti-actin antibody. Quantification of MNNG-induced γ-H2AX foci formation in PARP-$1^{+/+}$ and PARP-$1^{-/-}$ MEF. Cells were treated with 50 μM MNNG, fixed and immunoassayed with anti-phospho-H2AX (serine 139) monoclonal antibody. Confocal microscopy images of γ-H2AX foci were counted at (*B*) 30 min, (*C*) 4 h, and (*D*) 8 h after MNNG treatment. For the determination of γ-H2AX foci per cell, multiple fields were examined to count at least 150 cells for each time point.

H2AX phosphorylation at serine 139 within the first hour of treatment with both MNNG and PJ-34 (Fig. 2*C*). Therefore, to determine whether PAR synthesis occurred predominantly at sites of γ-H2AX foci formation, we treated A549 cells with the alkylating agent MNNG and examined the colocalization between early γ-H2AX foci formation and PAR nuclear synthesis by indirect immunofluorescence. MNNG treatment caused a marked increase in phosphorylation of H2AX in a time-course similar to that of PAR synthesis (Fig. 2*D*). As seen in Fig. 2*D*, PAR colocalizes with sites of γ-H2AX foci formation. Collectively, these results strongly support the hypothesis that PAR is an early DNA damage signaling molecule that connects with ATM-signaling cascade.

PARP-1-deficient Cells Have an Impaired DNA Damage Response—It has been suggested earlier that enzymatic activity of PARP-1 is required for p53 stabilization (46–48). Therefore, we examined whether MEFs deficient in PARP-1 were also defective in early MNNG-induced DNA damage response as determined by p53 phosphorylation and stabilization. Phosphorylation of p53 is generally associated with its stabilization and nuclear accumulation (49). Accordingly, we show that PARP-1-deficient MEFs exhibit a severe deficiency in p53 phosphorylation (on serine 18 in mouse p53) and accumulation (Fig. 3*A*) consistent with the delayed phosphorylation of p53 observed in cells treated with a chemical inhibitor following MNNG treatment (Fig. 2*B*). Interestingly, the rapid ATM-dependent phosphorylation of SMC1 at serine 957 was also seriously impaired in PARP-1-deficient cells exposed to MNNG (Fig. 3*A*), confirming the defects observed with cells treated with PJ-34.

We have shown that sites of intense poly(ADP-ribosyl)ation colocalize with γ-H2AX in distinct nuclear foci generated by MNNG (Fig. 2*D*). Thus, to further define the requirement of PARP-1 activity in the early signaling of DNA damage formation, we investigated the kinetics of γ-H2AX foci formation in PARP-1-deficient MEFs following exposure to MNNG. Without MNNG treatment, γ-H2AX foci were barely detected in PARP-$1^{+/+}$ MEFs, but a small number of γ-H2AX foci could be observed in PARP-$1^{-/-}$ MEFs (data not shown). Although γ-H2AX foci formation was induced in both cell lines 30 min after MNNG treatment (Fig. 3*B*), the rate of γ-H2AX foci formation was markedly slower in PARP-$1^{-/-}$ cells, confirming the involvement of PARP-1 activity in signaling the presence of damaged DNA. Quantitative image analysis of γ-H2AX-positive cells showed that both cell lines have almost equal number of γ-H2AX foci, 4 h after MNNG exposure (Fig. 3*C*), suggesting that DNA damage-induced γ-H2AX foci formation is delayed but not completely abrogated in the absence of PAR formation. However, 8 h after MNNG treatment, cells lacking PARP-1 showed a marked increase in the number of cells positive for γ-H2AX foci, with about 65% of the cells containing more than 15 γ-H2AX foci per cell compared with 8% in

cells proficient in PARP-1 and subjected to the same treatment (Fig. 3*D*). These data suggest that enzymatic activity of PARP-1 is required to resolve DNA breaks induced by genotoxic agents.

Poly(ADP-ribosyl)ation Modifies the Effectiveness of the ATM-signaling Response Induced by Ionizing Radiation—The influence of poly(ADP-ribosyl)ation on DNA repair following IR has been studied in the past using potent PARP inhibitors (47, 48). In particular, it has been observed in various human cancer cell lines that inhibition of PAR synthesis enhance the cell-killing effect of γ-irradiation (19, 21). Although the molecular events associated with this increased cytotoxicity are unknown, several recent observations imply a role for poly(ADP-ribosyl)ation in the ATM/ATR signaling pathways. To test whether PAR synthesis is involved in this pathway, ATM-mediated phosphorylation of p53, SMC1, and H2AX was analyzed in γ-irradiated (10 Gy) cells treated with or without PJ-34. We first determined the time course of PAR formation following IR in these conditions (Fig. 4*A*). PAR synthesis peaked rapidly and declined within 15 min after IR for both normal and A-T cells, demonstrating the transient nature of poly(ADP-ribosyl)ation (Fig. 4, *A* and *B*). In contrast, negligible PAR synthesis could be detected in cells pretreated for 1 h with PJ-34 (Fig. 4, *A* and *B*). As expected, IR treatment also rapidly stimulated phosphorylation of the main ATM targets p53, SMC1, and H2AX (Fig. 4*A*). In contrast, cells treated with PJ-34 only show a limited phosphorylation of ATM effectors at early time points after IR (Fig. 4*A*). Although the effect was not as marked as that seen in MNNG-treated cells, we observed a significant delay in p53 serine 15 phosphorylation between 5 and 30 min after exposure to IR and PJ-34 (Fig. 4, *A* and *B*). As previously reported, the phosphorylation of p53 is almost exclusively dependent on ATM kinase activity at these early time point after irradiation (50). As a result, A-T cells exposed to IR do not exhibit phosphorylation of the ATM main targets p53, SMC1, and H2AX. Interestingly, treatment of cells with PJ-34 decrease the ATM-dependent phosphorylation of SMC1 to a level comparable with that observed in A-T cells (Fig. 4, *A* and *B*), suggesting a dependence between PAR and ATM in the initial response to IR. Moreover, following concomitant exposure to IR and PJ-34, the phosphorylation of H2AX at serine 139 is only one third of that measured 15 min after cells have been exposed to IR only (Fig. 4, *A* and *B*). To determine whether the ATM-dependent phosphorylation of H2AX in response to IR-induced DSBs is mediated in association with PAR synthesis, we directly evaluated the presence of PAR signal at DSB-flanking regions by indirect immunofluorescence using anti-γ-H2AX phosphospecific antibody. Again, PAR synthesis clearly spreads throughout DSB regions marked by γ-H2AX (Fig. 4*C*). These results thus suggest that the functional interplay between PAR and ATM prevails in DNA damage response induced by different types of damaging agents.

Poly(ADP-ribose) and ATM Physically Interact—The mechanism underlying the interplay between the early PAR-dependent signaling pathway and the activation of the DNA damage-responsive kinase ATM might be mediated by a direct interaction between ATM and PAR. Thus, to verify whether ATM directly binds PAR molecules, we used twelve overlapping GST-tagged ATM domains (Fig. 5*E*) (38) spanning the entire ATM protein in a quantitative *in vitro* PAR-binding assay. The GST-tagged N-terminal amino acid region (GST-ATM1; 1–246) and PI3K domain of ATM (GST-ATM10; 2427–2840) specifically bound PAR while the GST-tag alone did not (Fig. 5, *A–C*). As a positive control, core histones exposed to 100 nM of either modified PARP-1 or free PAR showed strong binding affinities (Fig. 5, *B* and *C*, *first lane*). To test whether PAR directly mediates the interaction between PARP-1 and ATM, we performed specific pull-down experiments using the GST-ATM fusion proteins that exhibited PAR binding activity. Both domains specifically interact with either poly(ADP-ribosyl)ated PARP-1 (Fig. 5*D*, *lanes 8* and *13*) or purified PAR (Fig. 5*D*, *lanes 10* and *15*) but fail to bind PARP-1 alone or modified PARP-1 after hydrolysis of PAR by poly(ADP-ribose) glycohydrolase (PARG) (Fig. 5*D*, *lanes 7*, *9*, *12*, and *14*, respectively). The presence of PARP-1 in GST precipitates was verified by Western blot using a monoclonal PARP-1 antibody (Fig. 5*D*). The fact that PARP-1 could not be detected in GST pull down with purified PARP-1 (Fig. 5*D*, *lanes 7* and *12*) or modified PARP-1 after PAR was hydrolyzed by PARG (Fig. 5*D*, *lanes 9* and *14*) clearly demonstrated that these ATM regions do not directly bind to PARP-1 unless it is poly(ADP-ribosyl)ated. These results support the idea that these two regions of the ATM protein might comprise a functional domain that mediates direct interaction with PAR.

ATM Has Two Putative PAR-binding Domains—Based on a previous report on PAR-binding proteins, we have determined key amino acids that dictate affinity and specificity for PAR interaction and identified two putative PAR-binding domains within these ATM regions (Fig. 5*E*). Typically, the PAR-binding domain comprises a core of 20 amino acids characterized by the presence of hydrophobic and determinant repeated basic residues flanked by noncontiguous basic residues that provide additional contact to PAR molecules (34, 51). The first putative PAR-binding domain extended from amino acids 99–120 of ATM (Fig. 5*E*) and is located in the chromatin-association domain (52). The second domain lies in the C-terminal region within amino acids 2738–2760, and partly overlaps the PI3K domain of ATM (Fig. 5*E*). Comparison of the putative ATM PAR-binding sites from human, mouse, and pig sequences shows that the N-terminal binding site (99–120) is highly conserved with the consensus sequence (Fig. 5*E*). As shown in a recent report, the N-terminal protein interaction domain of ATM resides specifically within amino acids 81–106 (53) and is essential for the interaction with and phosphorylation of p53 (38). Thus, the fact that ATM interacts with PAR molecules through its N-terminal domain, provides a functional link for cross-talk between PAR synthesis and ATM activation.

To demonstrate the affinity of these ATM PAR-binding domains to specifically bind PAR, small mimetic peptides corresponding to the putative PAR-binding domains (99–120 and 2738–2760) were designed (Fig. 6*A*). Previous studies have used synthetic peptides in a similar PAR-binding assay and demonstrated that several DNA damage proteins can specifically bind PAR (34, 54). The PAR binding assay showed that ATM 99–120 and ATM 2738–2760 peptides do indeed bind PAR *in vitro* (Fig. 6*B*). It has been suggested that PAR binding requires the presence of basic residues in the amino acid

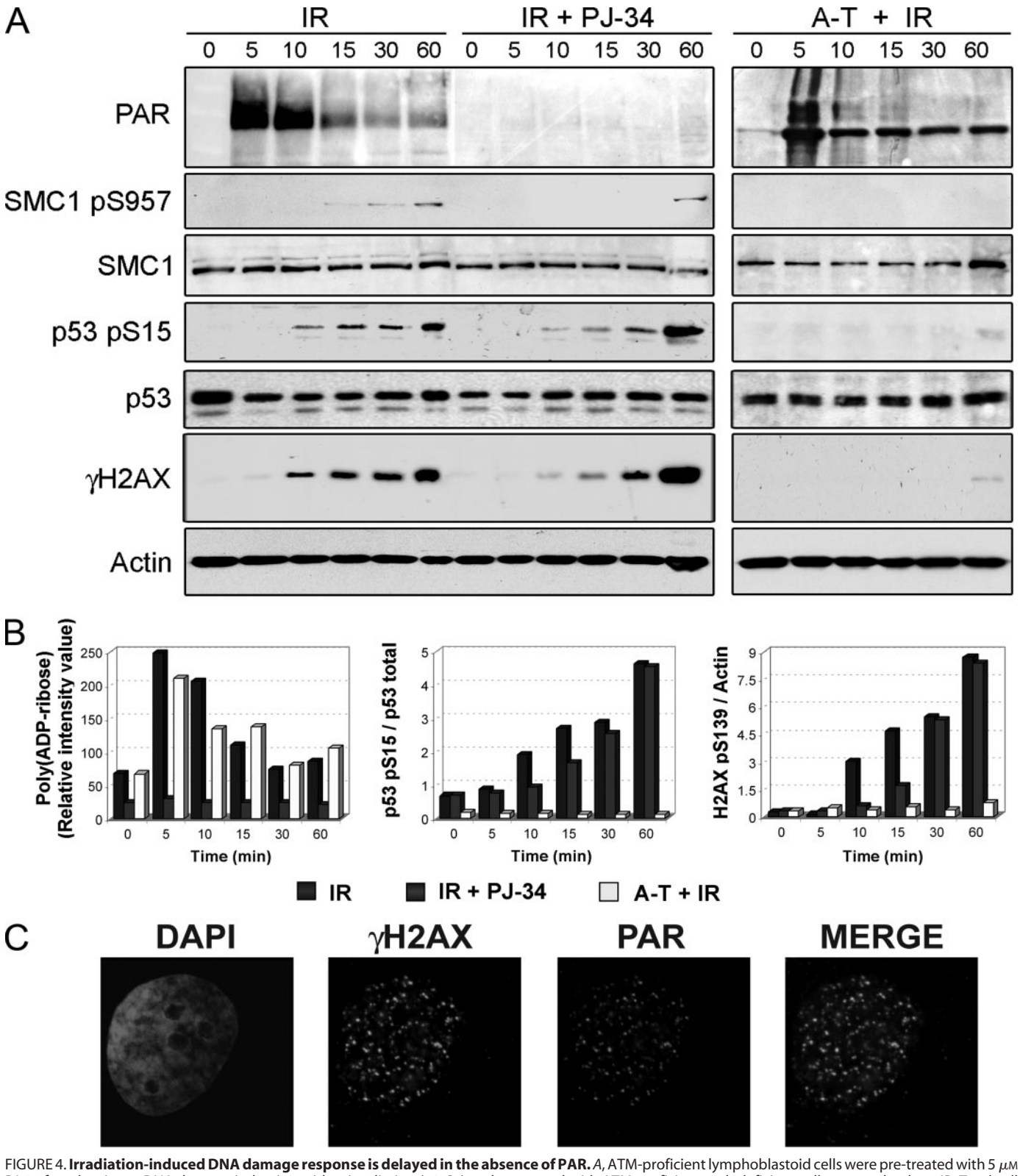

FIGURE 4. **Irradiation-induced DNA damage response is delayed in the absence of PAR.** *A*, ATM-proficient lymphoblastoid cells were pre-treated with 5 μM PJ-34 for 1 h prior to DNA damage induction with γ-irradiation (10 Gy) and compared with ATM-proficient and -deficient cells exposed only to IR. Total cell extracts where then immunoblotted with phosphospecific antibodies directed against known downstream effectors of ATM. *B*, densitometric quantification of PAR synthesis, p53 phosphorylation on serine 15, and γ-H2AX were performed directly on immunoblots shown in *A*. *C*, GM00637 cells were irradiated with 5 Gy and fixed within 5 min before immunostaining with anti-PAR and γ-H2AX antibodies. Data are representative of at least three independent experiments.

sequence (34, 51, 55). Hence, to determine whether any basic amino acid residues are required for ATM-PAR interaction, we took advantage of the binding affinity of the ATM peptide 99–120 in which the basic amino acids of the binding site were replaced by alanines. We observed that substitution of the basic repeat (ATM S3) or the C-terminal basic residues (ATM S4)

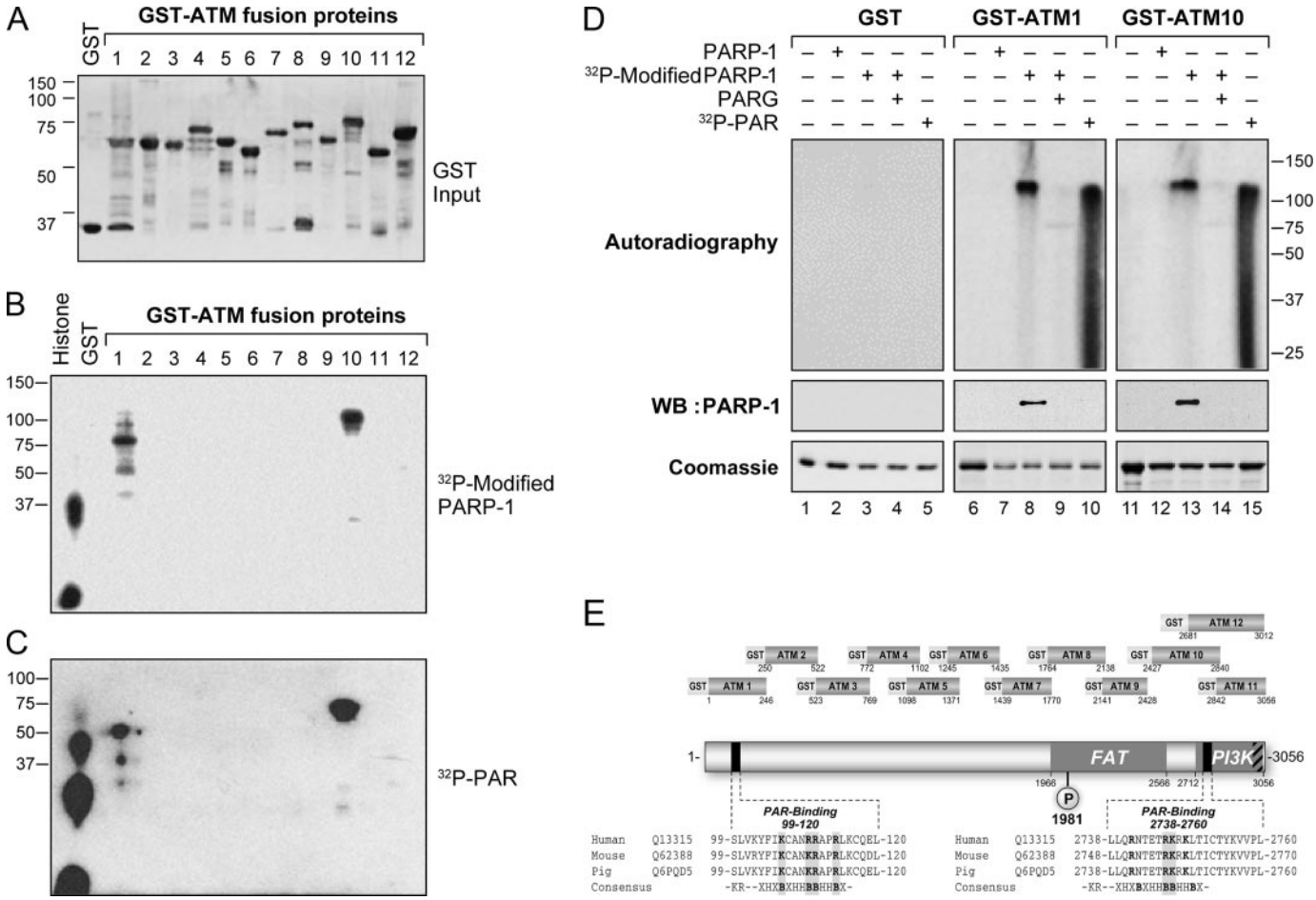

FIGURE 5. **Biochemical analysis of the interaction between ATM and PAR.** *A*, SYPRO Ruby Red protein blot staining of purified GST-ATM fusion proteins schematized in *E*. Autoradiography of PAR-binding GST-ATM fusion proteins incubated with 100 nM of either (*B*) ^{32}P-labeled automodified PARP-1 or (*C*) purified ^{32}P-labeled PAR. *D*, mapping of the region of ATM that interacts with PAR by pull-down assays with purified PARP-1, modified PARP-1 and PAR was performed as described under "Materials and Methods." Autoradiograms show the presence of PAR in the pull-down fraction. Detection of PARP-1 in the pull-down fraction was achieved by Western blotting. Coomassie Blue gel staining reveals the amount of precipitated GST-tagged protein. The *lanes 1*, *6*, and *11* represent purified GST protein input. *E*, schematic representation of the series of GST-ATM constructs (38). Shown below is the domain architecture of full-length ATM protein. The two putative PAR-binding sites are indicated in *black*. Alignment of human, mouse, and pig ATM sequences with the consensus PAR-binding domain is also shown. SwissProt accession numbers are provided. Conserved basic amino residues are indicated in *bold* against a *light gray* background.

considerably reduce the ability of substituted peptides to interact with PAR (Fig. 6, *B* and *C*). To explore the possible mechanism by which PAR affected the ATM function, we used a lipid-mediated formulation to achieved intracellular delivery of peptides derived from the N-terminal PAR-binding domain of ATM protein kinase (ATM 99–120) in intact cells (40, 41). After intracellular delivery of the PAR-binding peptide ATM 99–120, phosphorylated ATM was easily detectable by immunostaining. Although these cells exhibited normal levels of autophosphorylated ATM, they are defective for foci formation (Fig. 6*D*). Notably, this effect has not been observed for the recruitment of other DSB sensors at DNA damage sites including 53BP1 (Fig. 6*E*). Most importantly, the administration of PAR-binding peptides, where important basic residues were substituted by alanine (ATM S4), failed to disrupt ATM pS1981 foci formation under the same condition (Fig. 6*D*). To test whether the ATM 99–120 peptide has an influence on ATM mediated downstream processes, the phosphorylation of p53 on serine 15 was studied. After treatment with MNNG (50 μM, 1 h), cells treated with ATM 99–120 peptide exhibited a noticeable dose-dependent reduction of p53 phosphorylation, whereas levels of p53 phosphorylation in cells treated with ATM S4 peptide was largely unchanged (Fig. 6*F*). The immunofluoresence results combined with Western blotting data clearly suggest that ATM is activated following MNNG treatment and that intracellular delivery of the ATM 99–120 peptide preclude the accumulation of phosphorylated ATM at DNA damage sites. The quantitative decrease of ATM-dependent p53 phosphorylation observed by immunoblot after treatment with the ATM 99–120 peptide is likely related to this mislocalization of autophosphorylated ATM. Thus, specific binding to PAR does not seem to be required for the initial activation of ATM, but rather appear to play an important role in recruiting activated ATM to the sites of DNA breaks, where it can then phosphorylate substrates, including p53, SMC1, and H2AX. These observations suggest that the abnormal DNA damage response seen in cells with impaired PAR synthesis result from a defective ATM migration to sites of DNA breaks. Our results subsequently imply that optimal activa-

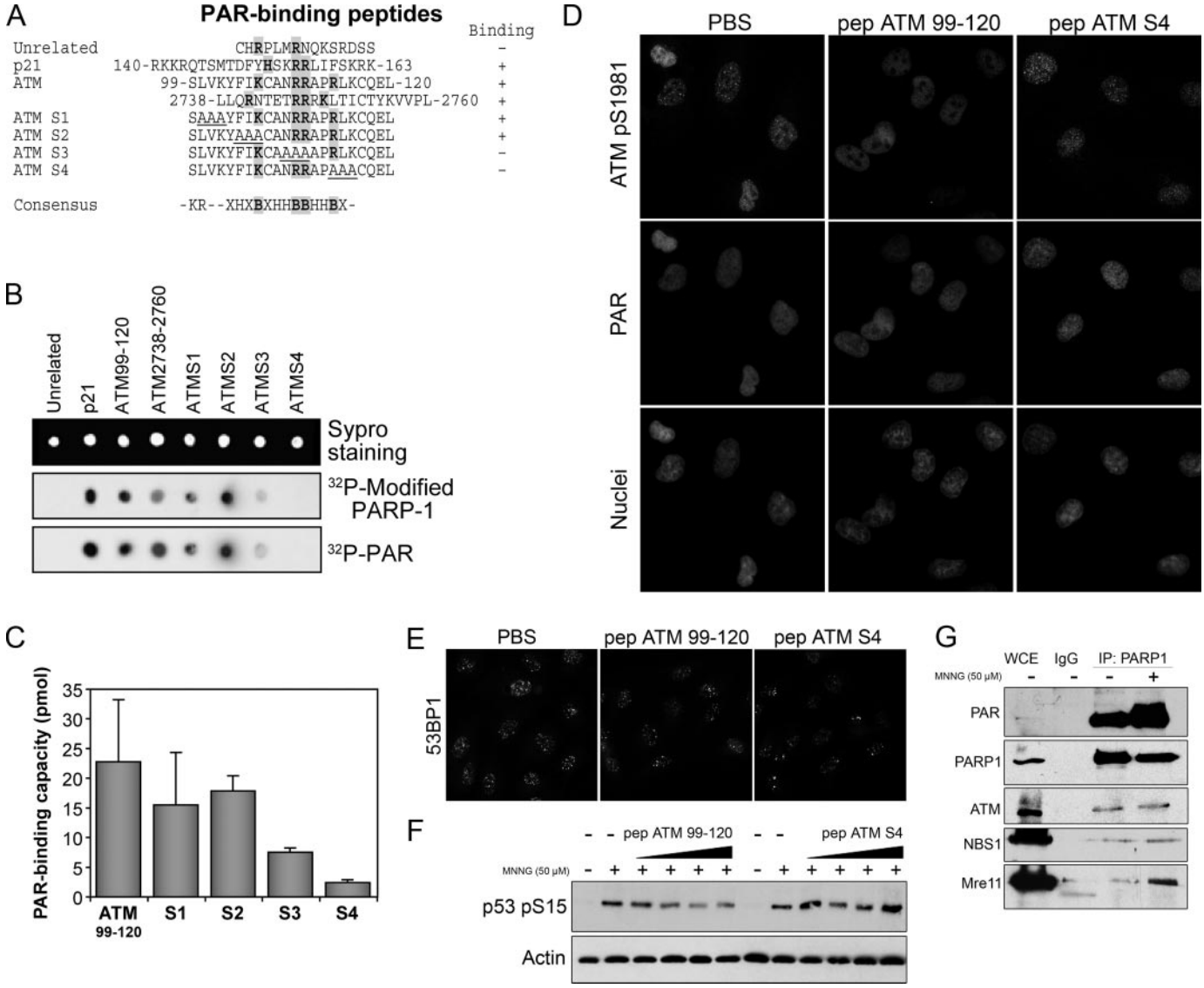

FIGURE 6. **Identification of functional PAR-binding sites within ATM protein kinase.** *A*, synthetic mimetic peptides corresponding to the putative PAR-binding motif of ATM were generated with or without alanine substitutions. Conserved basic residues are indicated in *bold* against a *light gray* background. *B*, indicated peptides were blotted onto nitrocellulose membrane and analyzed for PAR binding affinity. p21 peptide was used as a positive control (34) and a short unrelated peptide sequence was the negative control. The *upper panel* shows a SYPRO Ruby Red staining of blotted peptides and confirms equal loading. The *middle panel* shows that ATM PAR-binding motif peptide binds to 100 nM equivalent of PAR amount covalently attached to PARP-1. The *lower panel* presents the nitrocellulose PAR binding assay in the presence of purified 100 nM ^{32}P-labeled PAR. *C*, PAR binding capacity of ATM99–120 peptide and alanine-substituted peptides (ATMS1 to ATM S4) was quantified using Cerenkov counting of ^{32}P-labeled free PAR bound to nitrocellulose. *D*, defective foci formation of DSB repair molecules in cells treated with PAR-binding mimetic peptides. Mimetic peptides (2.5 μg) were introduce in human adenocarcinoma cells A549 using the BioPorter delivery system 4 h before treatment with 50 μM MNNG. Following MNNG treatment, the DNA damage-induced activation of ATM was monitored by serine 1981 autophosphorylation at 30 min and correlates with PAR synthesis detected using anti-PAR antibody. *E*, foci formation of DSB-sensing factor 53BP1 in cells treated with PAR-binding mimetic peptides. *F*, cells were treated with increasing amount of PAR-binding mimetic peptides and phosphorylation of the ATM downstream target p53 was monitored by Western blotting using p53 serine 15 phosphospecific antibody 30 min after MNNG treatement. Actin was used as a loading control. *G*, *in vivo* IP analysis of PARP-1 interaction with ATM protein kinase using C3ABR total cell extracts treated or not with 50 μM MNNG for 1 h.

tion of the ATM-mediated DNA damage response requires PAR synthesis.

Finally, we tested the possibility that PARP-1 might interact with the ATM signaling network *in vivo*. Intracellular interaction between PARP-1 and ATM has been identified by co-immunoprecipitation (IP) of endogenous PARP-1 protein followed by Western blotting detection of ATM (Fig. 6*G*). We also immunoprecipitated endogenous PARP-1 following MNNG treatment and determined the level of poly(ADP-ribosyl)ation using anti-PAR antibody (Fig. 6*G*). Of note, Mre11, a key component of MRN complex, was also found in the same IP and is present in a relatively higher amount in IPs from MNNG-treated cells (Fig. 6*G*). Collectively, these results demonstrate that ATM and PAR can physically interact together which is likely to be achieved by a specific PAR-binding domain.

DISCUSSION

DNA damage response pathways are essential for the maintenance of genomic integrity and mammalian cells have developed an intricate signaling network that allows the detection of

DNA lesions by sensors, leading to transduction of signals by effector proteins, resulting in the activation of checkpoint pathways that transiently arrest cell cycle progression to allow repair. A long standing question in the PARP field has been whether poly(ADP-ribosyl)ation is a true modulator of this early DNA damage signaling pathway. Evidence suggests that disruption of poly(ADP-ribosyl)ation metabolism by chemical inhibition or genetic disruption of PARP-1 significantly decreases cell survival, specifically in association with genetic disorders where homologous recombination (HR) is compromised (8–10). Similarly, cells with impaired ATM function are characterized by hypersensitivity to DSB-inducing agents and are also defective for cell cycle checkpoint activation (43). In this work, we confirmed that reducing PAR synthesis by chemical inhibition markedly increased the sensitivity of normal cells to DNA-damaging agents (Fig. 1) and affected the activation of cell cycle checkpoint (supplemental Fig. S1). Given that failure in DNA damage-induced poly(ADP-ribosyl)ation causes defects similar to those associated with ATM deficiency, we hypothesized that the early PAR-dependent signaling response connects with the signaling pathways controlled by ATM. Therefore, using A-T cells, we observed that the PARP inhibitor PJ-34 significantly increased cell death with or without DNA damage (Fig. 1 and supplemental Fig. S1). This has been previously revealed in PARP-1/ATM double knock-out cells (26) and more recently in PARP-1-deficient cells treated with ATM inhibitors (10, 56). Importantly, in the range of treatment doses used in this study, PJ-34 alone did not display such toxicity in normal cells (Fig. 1*B*). Together, these results support the idea that PAR synthesis is involved in a functional interplay with the ATM signaling network.

Two groups have reported that PARP inhibitors used alone for long periods of time activate ATM, presumably through persistence of endogenous single strand breaks that have the potential to be converted to DSB during replication (10, 56). In contrast, in this study we investigated the effects of PARP inhibitors on the early signaling events that take place when ATM is activated by exogenous DNA lesions created by either MNNG or IR. Although not exclusive to ATM, several lines of evidence indicate that the phosphorylation of p53, SMC1, and H2AX is primarily achieved by the upstream kinase ATM in response to DNA damage induced by both IR and MNNG treatment (2, 50). Our results suggest that the rapid and transient PAR formation creates a unique signal that directly or indirectly results in activation of the ATM signaling pathway. Previous work has proposed that ATM is not activated directly by binding to DNA damage sites but rather by a signal generated by a structural change of chromatin (2, 50). Thus, PAR molecules attached to PARP-1 might act as a sensor and initiate a DNA damage response through modulation of the ATM signaling pathway. Accordingly, the PAR-binding domain identified here appears to have a notable function for recruiting activated ATM at sites of DNA breaks. Consequently, we demonstrate that in the absence of PAR synthesis, ATM-dependent phosphorylation of p53, SMC1, and H2AX is significantly reduced in cells treated with both MNNG and IR (Figs. 2 and 4). Notably, although the PARP-inhibited cells show a clear delay in phosphorylation of ATM substrates after MNNG or IR treatment, this effect is less prominent than the defect observed in a cell line deficient in ATM (Figs. 2 and 4). We could not exclude that ATR might be responsible for the phosphorylation of p53 and SMC1 at later time points (>1 h) in both PARP-inhibited and ATM-deficient cells. However, it is unlikely that ATR alone could mediate the early PAR-dependent response reported here, because no PAR-binding domain has been found within the ATR amino acid sequence. We clearly show that following either MNNG or IR treatments, PAR accumulation is rapid and effectively colocalizes with γ-H2AX (Figs. 2*D* and 4*C*), which is known to accumulate instantly after DNA damage in a manner that is closely related to numbers of DSB (44). Our results are consistent with recent studies showing that PARP-1 predominantly localizes to DSB sites induced by microbeam irradiation (57) and directly interacts with γ-H2AX in response to IR (58). However, we noticed a delayed accumulation and a longer persistence of γ-H2AX foci in PARP-$1^{-/-}$ cells in response to genotoxic exposure (Fig. 3), presumably reflecting a defect in the DNA damage repair pathway.

To our knowledge, we are the first group to demonstrate and characterize a direct interaction between ATM and PAR using both GST fusion domains of ATM and specific peptides mimicking ATM PAR-binding domains (Figs. 5 and 6). GST-pull downs specifically show that ATM will bind to PARP-1 exclusively when PAR is present (Fig. 5*D*). Moreover, using small peptides which were expected to mimic the ATM 99–120 and ATM 2738–2760 PAR-binding domains, we confirmed experimentally that ATM does indeed bind PAR *in vitro* through those sequences (Fig. 6*B*). In contrast, peptides carrying mutations in critical basic positions of PAR-binding domain ATM 99–120 (ATM S3 and ATM S4) lost their affinity for PAR (Fig. 6, *B* and *C*). Furthermore, introduction of wild-type ATM PAR-binding peptides (ATM 99–120) in living cells disrupted the focus formation of phosphorylated ATM but not of other DSB repair molecules in cells treated with MNNG, while a mutant peptide had no effect on focus formation under the same conditions (Fig. 6, *D* and *E*). Disrupting the ATM-PAR interaction using PAR-binding mimetic peptides prevents the proper localization of ATM to DNA breaks and partially compromises the phosphorylation of p53 in response to DNA damage (Fig. 6*F*). Because it has been demonstrated that ATM is able to phosphorylate p53 even if it is not localized at DNA breaks (59), we observed only a partial protection of p53 phosphorylation in cells treated with the PAR-binding mimicking peptide ATM 99–120 (Fig. 6*F*). Consequently, the ability of ATM, as a mediator of the DNA damage response, to recognize PAR through a specific PAR-binding domain provides insight as to how noncovalent PAR interactions might alter the functional properties of its targets as observed following MNNG and IR treatments. Interestingly, the PAR-binding domain located within the N terminus of ATM (99–120) partially overlaps with the chromatin-association domain (5–224), which is required for ATM retention on chromatin and may target ATM to sites of DNA damage (52). In addition, the ATM N-terminal PAR-binding domain is highly conserved among species (Fig. 5*E*) and its importance is highlighted by the fact that no mutation has been reported within this sequence in A-T patients, supporting a link between PAR-binding and ATM functions. Overall, these

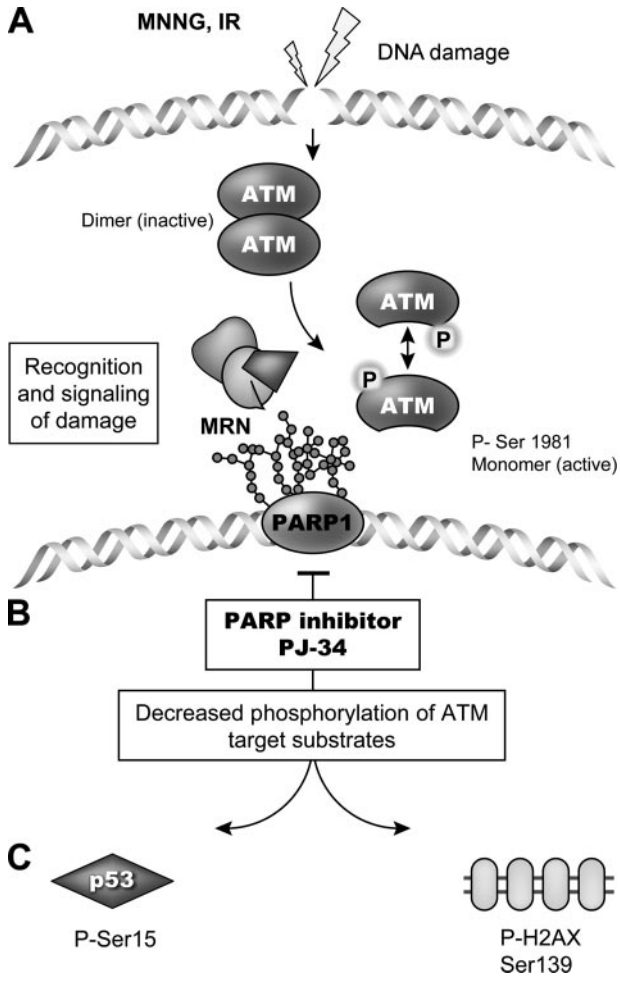

FIGURE 7. **Proposed model of interplay between ATM- and PAR-dependent signaling networks.** *A*, DNA strand breaks activate ATM and PARP-1. *B*, accumulation of PAR at sites of DNA damage probably contributes to the mobilization of ATM at DNA-damaged sites and ensuring phosphorylation of its downstream targets. *C*, decreased accumulation of PAR resulting from inhibition of PARP activity alters the kinetics of ATM-dependent substrates phosphorylation.

results confirm that ATM and PAR interact together in a noncovalent way via PAR-binding domains and support the conclusion that PAR is involved in the modulation of the DNA damage response through direct interaction with signaling proteins.

The physical association between ATM and PAR might explain the functional consequences of PARP inhibition observed *in vivo*. Incidentally, it was recently reported that PAR activates ATM *in vitro* (35). In that study, Goodarzi and Lees-Miller showed biochemically that PAR greatly stimulates ATM kinase function. Although it remains unclear whether PAR directly activates ATM *in vivo*, it is reasonable to envisage a model where the presence of PAR on modified proteins or on PARP-1 facilitates the phosphorylation of ATM downstream targets at sites of DNA damage. This in turn allows the induction of a proper DNA damage response upon genotoxic exposure (Fig. 7). Disrupting this interaction using PARP inhibitors undeniably interferes with the early DNA damage-induced phosphorylation of ATM downstream targets.

It is becoming clear that PAR synthesis provides a dynamic and transient mechanism that may be able to delicately modulate the activity of ATM protein kinase in cells treated with various DNA-damaging agents. The fact that the phosphorylation of ATM substrates is significantly delayed in the absence of PAR but still occurs suggests that other redundant pathways could contribute to the recruitment of ATM to specific sites of damaged DNA. Recent studies by Lee and Paull (60) suggest an important role for the MRN complex as a DNA damage sensor complex essential to the recruitment of ATM at sites surrounding damaged DNA. However, our results also suggest a unique synergy between ATM and poly(ADP-ribosyl)ation in the initial steps of DNA damage signaling. Identification of poly(ADP-ribosyl)ation as a critical event in this pathway constitutes an important issue to address in future studies on genetic disorders that are characterized by defective DNA damage responses and cancer predisposition.

Acknowledgments—We thank Michèle Rouleau and Danièle Poirier for critical reading of this manuscript. We also thank Marie-Eve Bonicalzi for technical assistance with the confocal microscope.

REFERENCES

1. O'Driscoll, M., and Jeggo, P. A. (2006) *Nat. Rev. Genet.* **7,** 45–54
2. Bakkenist, C. J., and Kastan, M. B. (2003) *Nature* **421,** 499–506
3. Lavin, M. F., Birrell, G., Chen, P., Kozlov, S., Scott, S., and Gueven, N. (2005) *Mutat. Res.* **569,** 123–132
4. Adamson, A. W., Kim, W. J., Shangary, S., Baskaran, R., and Brown, K. D. (2002) *J. Biol. Chem.* **277,** 38222–38229
5. Beardsley, D. I., Kim, W. J., and Brown, K. D. (2005) *Mol. Pharmacol.* **68,** 1049–1060
6. Stojic, L., Cejka, P., and Jiricny, J. (2005) *Cell Cycle* **4,** 473–477
7. Bouchard, V. J., Rouleau, M., and Poirier, G. G. (2003) *Exp. Hematol.* **31,** 446–454
8. Bryant, H. E., Schultz, N., Thomas, H. D., Parker, K. M., Flower, D., Lopez, E., Kyle, S., Meuth, M., Curtin, N. J., and Helleday, T. (2005) *Nature* **434,** 913–917
9. Farmer, H., McCabe, N., Lord, C. J., Tutt, A. N., Johnson, D. A., Richardson, T. B., Santarosa, M., Dillon, K. J., Hickson, I., Knights, C., Martin, N. M., Jackson, S. P., Smith, G. C., and Ashworth, A. (2005) *Nature* **434,** 917–921
10. McCabe, N., Turner, N. C., Lord, C. J., Kluzek, K., Bialkowska, A., Swift, S., Giavara, S., O'Connor, M. J., Tutt, A. N., Zdzienicka, M. Z., Smith, G. C. M., and Ashworth, A. (2006) *Cancer Res.* **66,** 8109–8115
11. Andrabi, S. A., Kim, N. S., Yu, S. W., Wang, H., Koh, D. W., Sasaki, M., Klaus, J. A., Otsuka, T., Zhang, Z., Koehler, R. C., Hurn, P. D., Poirier, G. G., Dawson, V. L., and Dawson, T. M. (2006) *Proc. Natl. Acad. Sci. U. S. A.* **103,** 18308–18313
12. Kim, M. Y., Zhang, T., and Kraus, W. L. (2005) *Genes Dev.* **19,** 1951–1967
13. Schultz, N., Lopez, E., Saleh-Gohari, N., and Helleday, T. (2003) *Nucleic Acids Res.* **31,** 4959–4964
14. Hochegger, H., Dejsuphong, D., Fukushima, T., Morrison, C., Sonoda, E., Schreiber, V., Zhao, G. Y., Saberi, A., Masutani, M., Adachi, N., Koyama, H., de Murcia, G., and Takeda, S. (2006) *EMBO J.* **25,** 1305–1314
15. Chalmers, A., Johnston, P., Woodcock, M., Joiner, M., and Marples, B. (2004) *Int. J. Radiat. Oncol. Biol. Phys.* **58,** 410–419
16. Lindahl, T., Satoh, M. S., Poirier, G. G., and Klungland, A. (1995) *Trends Biochem. Sci.* **20,** 405–411
17. Poirier, G. G., de Murcia, G., Jongstra-Bilen, J., Niedergang, C., and Mandel, P. (1982) *Proc. Natl. Acad. Sci. U. S. A.* **79,** 3423–3427
18. Malanga, M., and Althaus, F. R. (2005) *Biochem. Cell Biol.* **83,** 354–364
19. Calabrese, C. R., Almassy, R., Barton, S., Batey, M. A., Calvert, A. H., Canan-Koch, S., Durkacz, B. W., Hostomsky, Z., Kumpf, R. A., Kyle, S., Li,

J., Maegley, K., Newell, D. R., Notarianni, E., Stratford, I. J., Skalitzky, D., Thomas, H. D., Wang, L. Z., Webber, S. E., Williams, K. J., and Curtin, N. J. (2004) *J. Natl. Cancer Inst.* **96,** 56–67
20. Haince, J. F., Rouleau, M., Hendzel, M. J., Masson, J. Y., and Poirier, G. G. (2005) *Trends Mol. Med.* **11,** 456–463
21. Plummer, E. R. (2006) *Curr. Opin. Pharmacol.* **6,** 364–368
22. Noel, G., Godon, C., Fernet, M., Giocanti, N., Megnin-Chanet, F., and Favaudon, V. (2006) *Mol. Cancer Ther.* **5,** 564–574
23. Jacobson, E. L., Meadows, R., and Measel, J. (1985) *Carcinogenesis* **6,** 711–714
24. Shall, S., and de Murcia, G. (2000) *Mutat. Res.* **460,** 1–15
25. Menissier de Murcia, J., Ricoul, M., Tartier, L., Niedergang, C., Huber, A., Dantzer, F., Schreiber, V., Ame, J. C., Dierich, A., LeMeur, M., Sabatier, L., Chambon, P., and de Murcia, G. (2003) *EMBO J.* **22,** 2255–2263
26. Menisser-de Murcia, J., Mark, M., Wendling, O., Wynshaw-Boris, A., and de Murcia, G. (2001) *Mol. Cell Biol.* **21,** 1828–1832
27. Huber, A., Bai, P., Menissier-de Murcia, J., and de Murcia, G. (2004) *DNA Repair. (Amst.)* **3,** 1103–1108
28. Fang, Y., Liu, T., Wang, X., Yang, Y. M., Deng, H., Kunicki, J., Traganos, F., Darzynkiewicz, Z., Lu, L., and Dai, W. (2006) *Oncogene* **25,** 3598–3605
29. Chang, P., Coughlin, M., and Mitchison, T. J. (2005) *Nat. Cell Biol.* **7,** 1133–1139
30. Chang, P., Jacobson, M. K., and Mitchison, T. J. (2004) *Nature* **432,** 645–649
31. El-Khamisy, S. F., Masutani, M., Suzuki, H., and Caldecott, K. W. (2003) *Nucleic Acids Res.* **31,** 5526–5533
32. Leppard, J. B., Dong, Z., Mackey, Z. B., and Tomkinson, A. E. (2003) *Mol. Cell Biol.* **23,** 5919–5927
33. Malanga, M., and Althaus, F. R. (2004) *J. Biol. Chem.* **279,** 5244–5248
34. Pleschke, J. M., Kleczkowska, H. E., Strohm, M., and Althaus, F. R. (2000) *J. Biol. Chem.* **275,** 40974–40980
35. Goodarzi, A. A., and Lees-Miller, S. P. (2004) *DNA Repair. (Amst.)* **3,** 753–767
36. Wang, Z. Q., Auer, B., Stingl, L., Berghammer, H., Haidacher, D., Schweiger, M., and Wagner, E. F. (1995) *Genes Dev.* **9,** 509–520
37. Pandita, T. K., Lieberman, H. B., Lim, D. S., Dhar, S., Zheng, W., Taya, Y., and Kastan, M. B. (2000) *Oncogene* **19,** 1386–1391
38. Khanna, K. K., Keating, K. E., Kozlov, S., Scott, S., Gatei, M., Hobson, K., Taya, Y., Gabrielli, B., Chan, D., Lees-Miller, S. P., and Lavin, M. F. (1998) *Nat. Genet.* **20,** 398–400
39. Shah, G. M., Poirier, D., Duchaine, C., Brochu, G., Desnoyers, S., Lagueux, J., Verreault, A., Hoflack, J. C., Kirkland, J. B., and Poirier, G. G. (1995) *Anal. Biochem.* **227,** 1–13
40. Sawada, M., Hayes, P., and Matsuyama, S. (2003) *Nat. Cell Biol.* **5,** 352–357
41. Zelphati, O., Wang, Y., Kitada, S., Reed, J. C., Felgner, P. L., and Corbeil, J. (2001) *J. Biol. Chem.* **276,** 35103–35110
42. Beamish, H., Williams, R., Chen, P., and Lavin, M. F. (1996) *J. Biol. Chem.* **271,** 20486–20493
43. Shiloh, Y. (2006) *Trends in Biochemical Sciences* **31,** 402–410
44. Takahashi, A., and Ohnishi, T. (2005) *Cancer Letters* **229,** 171–179
45. Yu, Y., Zhu, W., Diao, H., Zhou, C., Chen, F. F., and Yang, J. (2006) *Toxicology in Vitro* **20,** 959–965
46. Wang, X., Ohnishi, K., Takahashi, A., and Ohnishi, T. (1998) *Oncogene* **17,** 2819–2825
47. Wieler, S., Gagne, J.-P., Vaziri, H., Poirier, G. G., and Benchimol, S. (2003) *J. Biol. Chem.* **278,** 18914–18921
48. Valenzuela, M. T., Guerrero, R., Nunez, M. I., Ruiz De Almodovar, J. M., Sarker, M., de Murcia, G., and Oliver, F. J. (2002) *Oncogene* **21,** 1108–1116
49. Appella, E., and Anderson, C. W. (2001) *Eur. J. Biochem.* **268,** 2764–2772
50. Canman, C. E., Lim, D. S., Cimprich, K. A., Taya, Y., Tamai, K., Sakaguchi, K., Appella, E., Kastan, M. B., and Siliciano, J. D. (1998) *Science* **281,** 1677–1679
51. Karras, G. I., Kustatscher, G., Buhecha, H. R., Allen, M. D., Pugieux, C., Sait, F., Bycroft, M., and Ladurner, A. G. (2005) *EMBO J.* **24,** 1911–1920
52. Young, D. B., Jonnalagadda, J., Gatei, M., Jans, D. A., Meyn, S., and Khanna, K. K. (2005) *J. Biol. Chem.* **280,** 27587–27594
53. Fernandes, N., Sun, Y., Chen, S., Paul, P., Shaw, R. J., Cantley, L. C., and Price, B. D. (2005) *J. Biol. Chem.* **280,** 15158–15164
54. Malanga, M., Pleschke, J. M., Kleczkowska, H. E., and Althaus, F. R. (1998) *J. Biol. Chem.* **273,** 11839–11843
55. Gagne, J. P., Hunter, J., Labrecque, B., Chabot, B., and Poirier, G. G. (2003) *Biochem. J.* **371,** 331–340
56. Bryant, H. E., and Helleday, T. (2006) *Nucleic Acids Res.* **34,** 1685–1691
57. Tartier, L., Spenlehauer, C., Newman, H. C., Folkard, M., Prise, K. M., Michael, B. D., Menissier-de Murcia, J., and de Murcia, G. (2003) *Mutagenesis* **18,** 411–416
58. Du, Y. C., Gu, S., Zhou, J., Wang, T., Cai, H., Macinnes, M. A., Morton Bradbury, E., and Chen, X. (2006) *Mol. Cell Proteomics* **5,** 1033–1044
59. Kitagawa, R., Bakkenist, C. J., McKinnon, P. J., and Kastan, M. B. (2004) *Genes Dev.* **18,** 1423–1438
60. Lee, J. H., and Paull, T. T. (2004) *Science* **304,** 93–96